

## Flow Dynamics in Growing Aneurysms

Shinobu Otsuka<sup>1</sup>, Hiroyuki Takao<sup>2</sup>, Yuichi Murayama<sup>2</sup>, Shunsuke Masuda<sup>2</sup>  
Ashraf Mohamed<sup>2,3</sup>, Yi Qian<sup>4</sup>, Masaya Suzuki<sup>5</sup>, Makoto Yamamoto<sup>5</sup>, Toshiaki Abe<sup>2</sup>

**1** Graduate School of Mechanical Engineering, Tokyo University of Science

1-14-6 Kudankita Chiyoda-ku Tokyo 102-0073 Japan, E-mail: j4510609@ed.kagu.tus.ac.jp

**2** Department of Neurosurgery, Jikei University School of Medicine

3-25-8 Nishishinbashi Minato-ku Tokyo, 105-8461 Japan, E-mail: takao@jikei.ac.jp, ymurayama@jikei.ac.jp, masuda\_s@jikei.ac.jp, abetoshi@jikei.ac.jp

**3** Siemens Japan K.K.

3-20-24, Higashi-Gotanda, Shinagawa-ku, Tokyo 141-8644 Japan, E-mail: ashraf.mohamed@siemens.com

**4** The Australian School of Advanced Medicine, Macquarie University

North Ryde 2109 Sydney, NSW Australia, E-mail: yi.qian@mq.edu.au

**5** Department of Mechanical Engineering, Tokyo University of Science

1-14-6 Kudankita Chiyoda-ku Tokyo 102-0073 Japan

E-mail: masaya@rs.kagu.tus.ac.jp, yamamoto@rs.kagu.tus.ac.jp

### Abstract

[Purpose] Subarachnoid Hemorrhage (SAH) is a serious disease which is fatal on onset in 30% of the patients. In 80% of the cases, SAH is caused by rupture of a cerebral aneurysm. As an aneurysm grows in size, its rupture risk increases. Hemodynamics is assumed to play an important role in aneurysm growth and rupture, and may therefore be used to assess the rupture risk. We performed unsteady hemodynamic simulations in three cases of cerebral aneurysms that grew during follow-up (one aneurysm ruptured). [Method] We performed CFD analysis with "ANSYS CFX 12.1" using the finite volume method. We studied hemodynamic changes before and after growth. In addition, we also investigated the aneurysms from the viewpoint of structural dynamics by performing structural analysis. [Result] Aneurysm growth causes a change in the flow ratio for diverging flows at MCA: decrease in ruptured case and increase in unruptured cases. Aneurysm growth causes a decrease in EL. Maximum Von Mises Stress is elevated at aneurysm neck and its value at the growth point is lower than the surrounding area.

**Keywords:** Cerebral aneurysm, growth, CFD

### Introduction

Subarachnoid Hemorrhage (SAH) is a serious disease which is fatal on onset in 30% of the patients. In 80% of the cases, SAH is caused by rupture of a cerebral aneurysm. Cerebral aneurysm is a disease in which the arterial wall locally bulges to form bump-like structure. Recently, early detection of unruptured aneurysms became possible due to the development of Computed Tomography Angiography (CTA) and Magnetic Resonance Imaging (MRI). To avoid aneurysm rupture, a medical operation is necessary, for example surgical clipping, which involves opening the cranial bone, or endovascular coiling which is relatively, less-invasive. Both operation types involve high risk, high cost burden, and high mental burden for patients. Not all cerebral aneurysms will rupture and it is known that the rupture risk is generally about 1%. There are big aneurysms which don't rupture. Furthermore there are aneurysms which grow and don't rupture. Generally when the

aneurysm size is more than 5mm, risk of rupture of the aneurysm is high. It is assumed that as aneurysms grow and increase in size, their rupture risk increases. It is thought that understanding growth mechanism of aneurysm will enable the understanding of the factors contributing to aneurysm rupture.

Recently Computational Fluid Dynamics (CFD) has attracted attention in a medical field and there are various CFD studies on cerebral aneurysms. Various combined factors are related to the rupture, occurrence, and growth of aneurysm, for example aneurysms shape, location, life style of the patient (history of smoking etc.), inheritable characteristics (SAH history of the family). Among them, hemodynamics is assumed to play an important role in aneurysm growth and rupture, and may therefore be used to assess the rupture risk. We performed unsteady hemodynamic simulations using the 3D models obtained from CTA for three cases of cerebral aneurysms that grew during follow-up (one aneurysm ruptured) and we studied

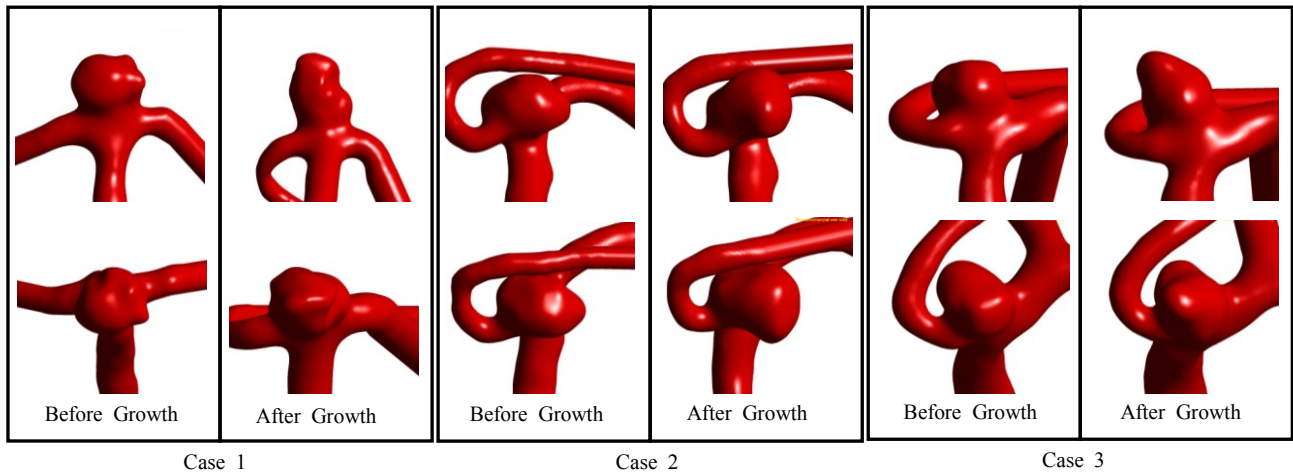


**Fig.1 Aneurysm structure before and after growth**

hemodynamic changes before and after growth. In addition, we also investigated the aneurysms from the viewpoint of structural dynamics by performing structural analysis.

**Methods**

*Patient Model*

We performed CFD simulations using 3D models obtained from CTA for three cases of Middle cerebral artery aneurysms (MCA) before and after growth during follow-up (one aneurysm ruptured during follow-up). Case 1 is ruptured aneurysm with height increase of 102.3%, during growth and period between before and after growth is 12 month. Case 2 is an unruptured aneurysm with height increase of 91.1% and period between before and after growth is 12 month. Case 3 is an unruptured aneurysm with height increase of 50.9% (formation of bleb) and period between before and after growth is 49 month. Table.1 and Figure.1 show the details of the shape for each case.

**Table 1**

		Height [mm]	Width [mm]	Neck [mm]	Time [month]
Case1	Before	3.09	4.34	3.68	12
	After	6.25	5.22	4.70	
Case2	Before	2.47	5.13	4.93	11
	After	4.72	5.82	5.20	
Case3	Before	2.93	5.45	4.46	49
	After	4.42	5.74	4.79	

*CFD Modeling*

The following is calculation process and method.

①Extracting aneurysm

The geometry of the arteries and aneurysm was extracted from Digital Imaging and Communication in

Medicine (DICOM) CTA images using "Real Intage" (Cybernet Systems). This geometry data was transformed into STL (Streolithography file format) and surface smoothing was performed using "Amira" (Visage Imaging). The portion of the blood vessels used in the simulation starts from the ICA and extends to the ACA and MCA after bifurcation.

②Constructing the computational mesh

We constructed the computational mesh from the smoothed STL data using "AMSYS ICEM CFD 12.1" (ANSYS). This CFD mesh is unstructured and consisted of mainly tetrahedral elements, with a fine and prismatic elements near the wall. The total number of elements in the mesh ranged from about 0.5 to 1.0 million. All inlets and outlets were extended 50 mm to avoid the negative effects of separation of flow or high curvature near the inlet and outlet surface.

③Computational condition

Laminar flow condition was assumed since the Reynolds number (characteristic length is Blood vessels diameter) is around 500. Inlet boundary condition was assumed to follow the mass flow rate profile<sup>[1]</sup> in Figure.2. Outflow boundary condition was fixed to 0 Pa. Rigid and non-slip boundary condition was assumed at the parent artery and aneurysm walls. The blood was assumed to be a Newtonian fluid with density and viscosity of 1,100 kg/m<sup>3</sup> and 0.0036 Pa · s respectively. This flow analysis was unsteady over two heartbeats (1.8 sec) with a time step of 0.5 msec. For initial conditions, a steady state solution was used, which was obtained with an inlet boundary condition of 0.00036 kg/s (initial value of the mass flow rate profile).

④Computational condition for structural analysis

Static analysis was performed. Initial load was set by pressure distribution which was the solution of steady CFD analysis and this inlet boundary was defined by average flow rate during heartbeat (0.008208 kg/s) and outlet boundary condition was fixed to 13435.6 Pa.

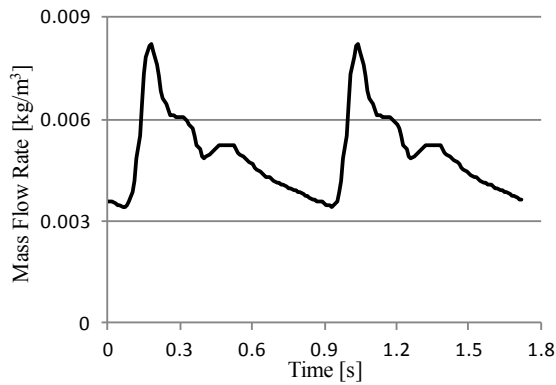


**Fig.2 Inlet Mass Flow**

Thickness of the blood vessel was assumed 0.3 mm and structural properties of vessel was assumed the same as silicon rubber (Young's modulus is 10.0 MPa, Poisson ratio is 0.3).

**Evaluation method**

Energy Loss (EL) was used to evaluate flow dynamics. EL indicate amount of energy loss of the flow through around the aneurysm. Computational volume and inlet plane and outlet plane for EL computation are shown Figure.3. Inlet and outlet planes were defined at a distance of 1 mm from aneurysm (Figure.3). EL is calculated from the average static pressure and velocity on the each surface according to the following equation

$$EL = \rho v_{in} A \left\{ \left( \frac{1}{2} \rho v_{in}^2 + P_{in} \right) - \left( \frac{1}{2} \rho v_{out}^2 + P_{out} \right) \right\}$$

where  $\rho$  [kg/m<sup>3</sup>] is density,  $v$  [m/s] and  $P$  [Pa] is average velocity and static pressure respectively. The subscripts "in" and "out" indicate the location where each parameter is computed, inlet a outlet plane respectively.

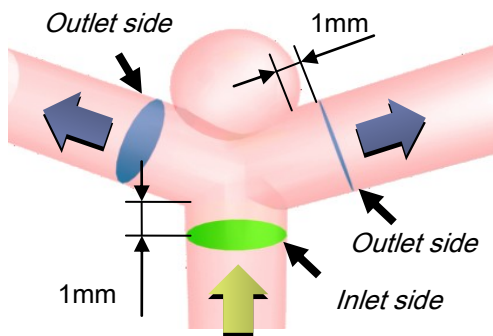


**Fig.3 Definition of Inlet or Outlet Area**

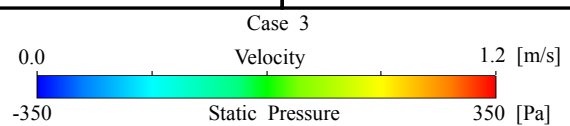
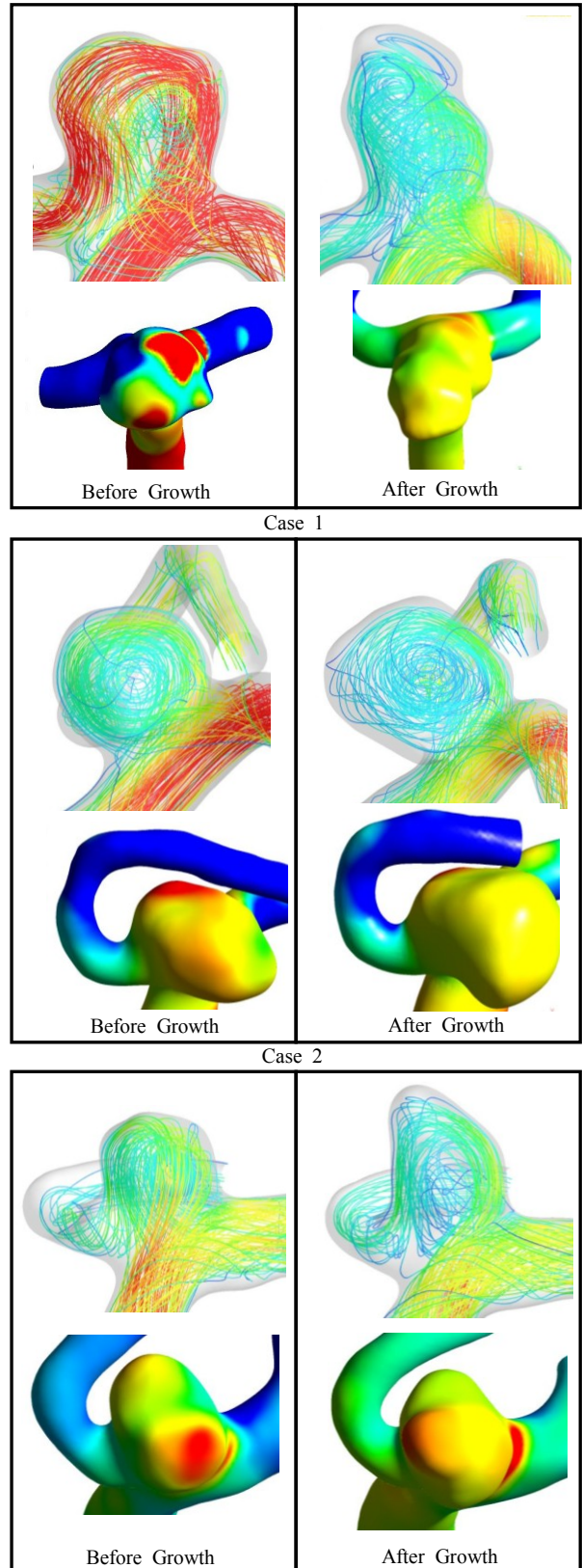


**Fig.4 Stream Line and Static Pressure Distribution**

## Results and discussion

### Transient flow

Firstly, the ratio of flow in the smaller blood vessel after the MCA bifurcation to the total flow is shown in Table.2. In Case1 (ruptured case), the flow ratio after growth decreases by 24.8%: the flow ratio to bigger vessel increases and to smaller vessel decreases. On the other hand, the flow ratios after the growth increase by 9.28% and 1.73 % in Case2 and Case3 respectively.

Figure.4 shows streamline and static pressure distributions at peak stroke. Colors on the streamline correspond to magnitude of the velocity vector. Static pressure is gauge pressure and its range is 700 Pa. High static pressure is shown in figure.4 at the impact area that is shown by streamline before growth. However, this high pressure area doesn't always correspond to the region which aneurysm grows at. In Case1, Static pressure on growth area is lower than the surrounding area. In Case2, the high pressure area is located on the opposite side of growth area. In Case3, location of high pressure area corresponds to that of growth area, but the direction of growth of bleb and the direction of impact as shown by streamline in figure.4 is different.

Table 2

Flow ratio	Case1	Case2	Case3
Before [%]	44.1	19.7	14.2
After [%]	19.4	29.0	15.9
Change ratio[%]	-24.8	9.28	1.73

Table 3

EL average	Case1	Case2	Case3
Before [ $\times 10^{-4}$ W]	16.82	5.84	5.53
After [ $\times 10^{-4}$ W]	2.81	3.50	4.14
Change ratio[%]	-83.3	-40.1	-25.2

Secondly, we compare EL before and after growth.

EL for each case is shown in Figure.5~7. In all cases, EL decreases after growth. Time averaged EL of each case is shown in Table.3. EL of of Case 1 (ruptured aneurysm) before growth is especially high. Shear Strain Rate (SSR) and surface streamline for each case at a cross-sectional plane in aneurysm is shown in figure.8. SSR before growth of Case 1 is very high at the shear layer which is the reason of high EL. Volume average SSR of each case at computational volume (between inlet and outlet surface in figure.3) is shown in Table.4. The table shows that the SSR for Case1 before growth is two times higher or more than in the other cases.

Table 4

Shear Strain Ratio	Case1	Case2	Case3
Before [ $s^{-1}$ ]	1703.7	769.0	739.2
After [ $s^{-1}$ ]	486.3	458.1	527.4
Change ratio [%]	-71.5	-40.4	-28.7

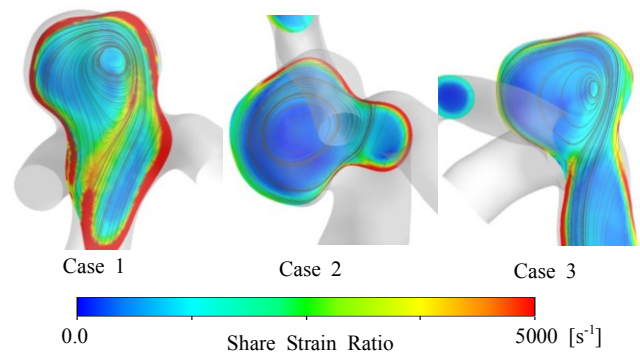


Fig.8 Shear Strain Ratio and Surface Stream Line in Aneurysm Before Growth

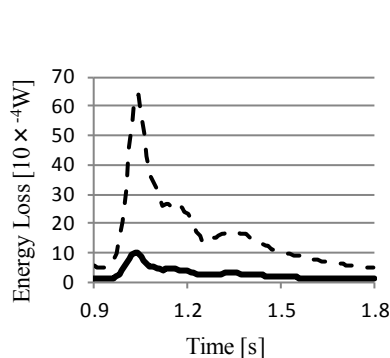


Fig.5 Energy Loss in Case 1

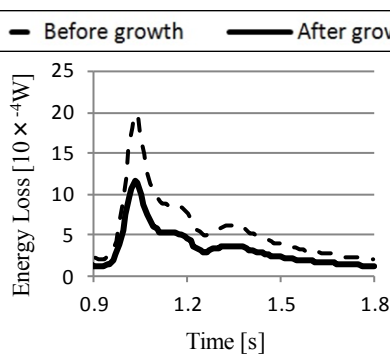


Fig.6 Energy Loss in Case 2

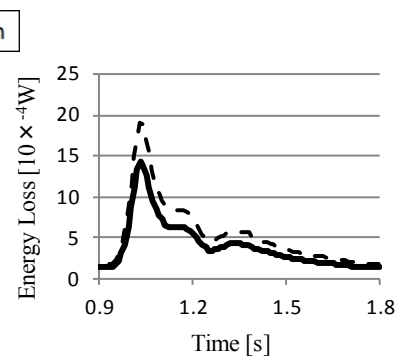
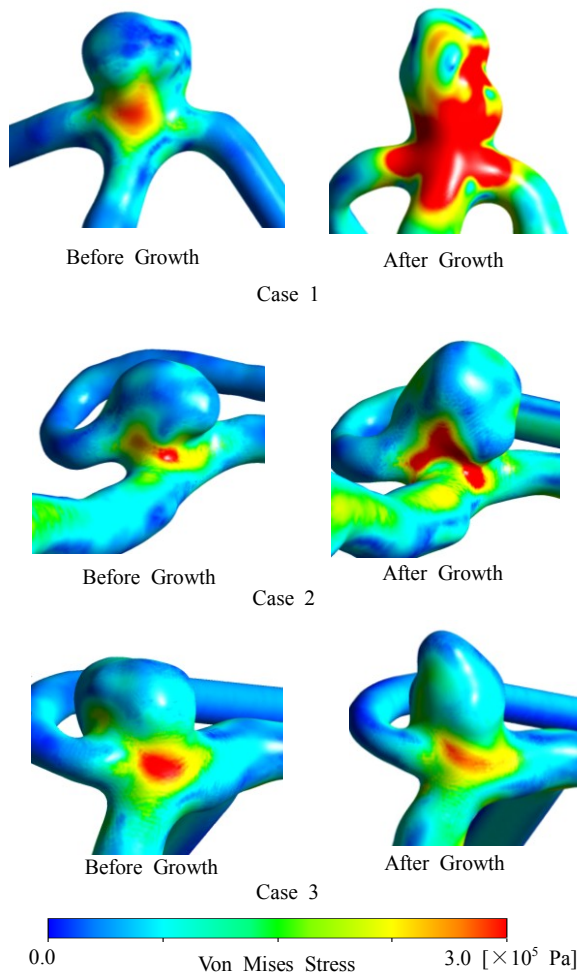


Fig.7 Energy Loss in Case 3



*Structural Analysis*

Figure.9 shows the Von Mises Stress distribution which is calculated through structural analysis. Von Mises Stress is highest at neck of aneurysm. Table.5 shows the maximum Von Mises Stress on the computational volume (which is the volume between the inlet and outlet planes defined in figure.3). In figure 9 and table 5, High Von Mises Stress is shown at aneurysm neck and it is elevated extremely after growth in Case1 (ruptured Case). The Von Mises Stress before growth near the growth area is about 0.197, 0.308, 0.239 [ $\times 10^{-5}$  Pa] for Case 1, 2, and 3 respectively. These values are one order lower than the maximum Von Mises Stress at neck of aneurysm. The Von Mises Stress distribution at growth area is shown in Fig.6 and growth point is circled. Von Mises Stress at growth point is lower than its surrounding area. From this result, it can be deduced that, counter to simple intuition, high force (stress) is not a cause of growth of aneurysm



**Fig.9 Von Mises Stress Distribution**

**Table 5**

Max Von Mises Stress	Case1	Case2	Case3
Before [ $\times 10^5$ Pa]	3.21	3.52	3.28
After [ $\times 10^5$ Pa]	6.95	5.15	3.32
Change ratio[%]	116.6	46.1	1.35

**Conclusion**

We performed CFD and Structural analysis for 3 aneurysms before and after growth and the following findings were obtained.

- (1) Aneurysm growth causes a change in the flow ratio for diverging flows at MCA: the flow ratio to bigger vessel increases and it to smaller vessel decreases in unruptured cases.
- (2) The locations of the impact area of flow and growth area of aneurysm are different.
- (3) Static pressure at growth area in aneurysm after growth is higher than the surrounding area.
- (4) Aneurysm growth causes a decrease in EL.
- (5) Maximum Von Mises Stress is elevated at aneurysm neck and its value at the growth point is lower than the surrounding area.

**References**

[1] Matthew, D. F., Noam, A. Sung, H. L., David W H., David, A. S., "Characterization of volumetric flow rate waveforms in the normal internal carotid and vertebral arteries," *Physiol. Meas.*, 26 (2005), pp. 477-488.

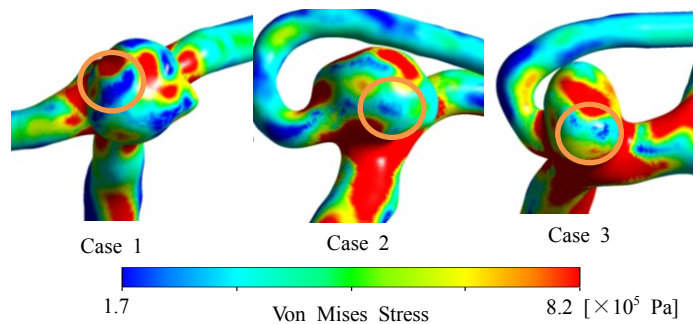


**Fig.10 Von Mises Stress Distribution at Growth Point on Aneurysm Before Growth**